

Accounting for uncertainty in dormant life stages in stochastic demographic models

Maria Paniw, Pedro F. Quintana-Ascencio, Fernando Ojeda and Roberto Salguero-Gómez

M. Paniw (maria.paniw@uca.es) and F. Ojeda, Depto de Biología - ceiA3, Univ. de Cadiz, Campus Río San Pedro, ES-11510 Puerto Real, Spain. – P. F. Quintana-Ascencio, Dept of Biology, Univ. of Central Florida, Orlando, FL 32816, USA. – R. Salguero-Gómez, Dept of Animal and Plant Sciences, Univ. of Sheffield, Sheffield, UK, and: Centre for Biodiversity and Conservation Science, Univ. of Queensland, QLD, Australia.

Dormant life stages are often critical for population viability in stochastic environments, but accurate field data characterizing them are difficult to collect. Such limitations may translate into uncertainties in demographic parameters describing these stages, which then may propagate errors in the examination of population-level responses to environmental variation. Expanding on current methods, we 1) apply data-driven approaches to estimate parameter uncertainty in vital rates of dormant life stages and 2) test whether such estimates provide more robust inferences about population dynamics. We built integral projection models (IPMs) for a fire-adapted, carnivorous plant species using a Bayesian framework to estimate uncertainty in parameters of three vital rates of dormant seeds – seed-bank ingress, stasis and egression. We used stochastic population projections and elasticity analyses to quantify the relative sensitivity of the stochastic population growth rate ($\log \lambda_t$) to changes in these vital rates at different fire return intervals. We then ran stochastic projections of $\log \lambda_t$ for 1000 posterior samples of the three seed-bank vital rates and assessed how strongly their parameter uncertainty propagated into uncertainty in estimates of $\log \lambda_t$ and the probability of quasi-extinction, $P_q(t)$. Elasticity analyses indicated that changes in seed-bank stasis and egression had large effects on $\log \lambda_t$, across fire return intervals. In turn, uncertainty in the estimates of these two vital rates explained > 50% of the variation in $\log \lambda_t$ estimates at several fire-return intervals. Inferences about population viability became less certain as the time between fires widened, with estimates of $P_q(t)$ potentially > 20% higher when considering parameter uncertainty. Our results suggest that, for species with dormant stages, where data is often limited, failing to account for parameter uncertainty in population models may result in incorrect interpretations of population viability.

Variation is the rule, rather than the exception, in natural settings (Tuljapurkar 1990, Boyce et al. 2006, Morris et al. 2008, Ehrlén et al. 2016). Selection pressures have emerged that shape strategies maximizing the passing on of genes to the next generation in the light of such a variation (Benton and Grant 1996, Smallegange and Coulson 2013). Dormancy is a life history strategy allowing organisms to avoid stress (Grime 1977) via sporulation in microorganisms (Pozzi et al. 2015), diapause in some animals (Schiesari and O'Connor 2013), or persistent seed banks in many plants (Doak et al. 2002). In the latter, seeds delay germination under environmental unpredictability, compensating for the risk of mortality associated with other stages through time (Cohen 1966, Venable 2007).

Persistent seed banks play a crucial role in the viability of many plant populations (Baskin and Baskin 1998, Doak et al. 2002), including in rare and invasive species (Adams et al. 2005, Gioria et al. 2012). Seed dormancy typically evolves in habitats where important events, such as precipitation (Gremer and Venable 2014) or fires (Quintana-Ascencio et al. 2003, Menges and Quintana-Ascencio

2004), are unpredictable. In these habitats, plant species with high temporal variation in reproductive output and high risk of reproductive failure with increasing environmental stochasticity typically produce dormant seeds (Baskin and Baskin 1998, Venable 2007, Tielbörger et al. 2012). The resulting seed banks may buffer against environmental stochasticity (Cohen 1966, Rees et al. 2006) and, in turn, against genetic drift (Honnay et al. 2008). Therefore, seed banks are of great interest in ecological and evolutionary processes because they may provide an important link between environmental stochasticity and population viability.

Understanding how seed banks influence population dynamics in stochastic environments is crucial to accurately project population trends (Menges 2000, Adams et al. 2005). Plant species with persistent seed banks may optimize fitness in stochastic environments by decoupling two key demographic processes: reproduction and survival-dependent growth (Doak et al. 2002). On the one hand, seeds that enter (ingress) and remain dormant (stasis) in the seed bank do not contribute to immediate germination and

aboveground growth, therefore lowering apparent short-term population growth rate estimates ($\hat{\lambda}$). On the other hand, germination (egression) from the seed bank can be triggered by environmental cues at a later time (Venable 2007), thus increasing $\hat{\lambda}$. Failing to accurately describe seed-bank transitions and the uncertainty around related parameters may therefore result in flawed estimates of projected population growth rates and extinction probability (Higgins et al. 2000, Doak et al. 2002).

Parameter uncertainty in general has been shown to contribute substantially to uncertainty in stochastic population models including dormant stages. However, the specific contributions to this uncertainty of vital-rate parameters describing seed-bank transitions remain little explored (Evans et al. 2010, Elderd and Miller 2016). In part, this is due to the difficulty of obtaining data for such vital rates, which results in models omitting, using simplified, or using latent (unobserved) parameters (Doak et al. 2002, Evans et al. 2010). Obtaining long-term seed-bank data is challenging for two reasons: 1) seeds may persist in the soil for periods far exceeding our own lifespans (Shen-Miller et al. 1995), and 2) due to their typically small size, tracking the fates of individual seeds in natural habitats without disrupting the soil is currently a nearly impossible task (Baskin and Baskin 1998, Navarra and Quintana-Ascencio 2012). Consequently, even if data on seed banks are collected, researchers usually extrapolate their long-term fates (Fig. 1) from short-term field experiments or models (Menges 2000). These approaches are sensitive to parameter uncertainty due to relatively small sample sizes and must account for this uncertainty when estimating population dynamics.

Here we show that in population models incorporating limited data on critical vital rates describing seed-bank transitions, the related parameter uncertainty alone (independent of other vital rates) may contribute greatly to the uncertainty around estimates of stochastic population

dynamics. Therefore, incorporating parameter uncertainty into stochastic simulations will significantly improve demographic interpretations. Using the fire-adapted carnivorous *Drosophyllum lusitanicum* (Drosophyllaceae) as a case study, we quantified how parameter uncertainty in seed-bank dynamics affected the potential interpretation of population-level responses to changes in fire regimes. The role of the seed bank is not well known for the study species, but we expected related vital rates to play a critical role in the estimation of viability as has been shown for other fire-adapted species (Menges and Quintana-Ascencio 2004, Adams et al. 2005). Building on existing approaches to separate sources of variation (Evans et al. 2010, Elderd and Miller 2016), we developed Bayesian stochastic integral projection models (IPMs; Easterling et al. 2000, Ellner and Rees 2006) using census data for above-ground and limited experimental data for the seed-bank transitions. We used elasticity analyses to determine the relative sensitivity of the stochastic population growth rate, $\log \lambda_s$, to changes in the mean of the three seed-bank vital rates. We then used stochastic simulations of different fire return intervals and IPMs built from parameter samples of seed-bank vital rates to estimate nested levels of variation in $\log \lambda_s$, and assess the variation (uncertainty) in estimates of the probability of quasi-extinction, $P_q(t)$, among parameter samples. We provide R scripts to apply the models and simulations (Supplementary material Appendix 1). Our results have important implications for the use of models to understand complex life cycles (e.g. those including diapause, vegetative dormancy, or migration) where vital rate quantification from data may contain high uncertainty.

Material and methods

Study species

We used data from natural populations of the fire-adapted, carnivorous short-lived subshrub *Drosophyllum lusitanicum* (Drosophyllaceae), (*Drosophyllum* hereafter) to build IPMs. This species is endemic to the southwestern Iberian Peninsula and northern Morocco and is associated with fire-prone Mediterranean heathlands (Paniw et al. 2015). Natural heathlands burn every 40 years on average, but may burn as early as 10 years after fire or remain unburned for >70 years (Ojeda 2009, Plan INFOCA 2012). Burned stands recover to mature vegetation within 3–5 years following fires (Calvo et al. 2002), and shrubs outcompete above-ground *Drosophyllum* individuals (Paniw unpubl.). Plants flower in the second year after germination and produce hard-coated, pear-shaped seeds (2.48 cm \pm 0.1 SE in length; Salces-Castellano et al. 2016). Most seeds remain dormant in the soil, and mass germination occurs after fire (Correia and Freitas 2002, Supplementary material Appendix 2). Reproductive plants produce 9.1 (\pm 2.6) viable seeds per fruit and up to 66 fruits (6.0 \pm 0.3) per plant. Although viable dormant seeds can accumulate in vast numbers (Salces-Castellano et al. 2016), and populations persist largely as seeds in the soil in between fires (Paniw unpubl.), little is known about the importance of seed fates for population dynamics of this rare carnivorous species.

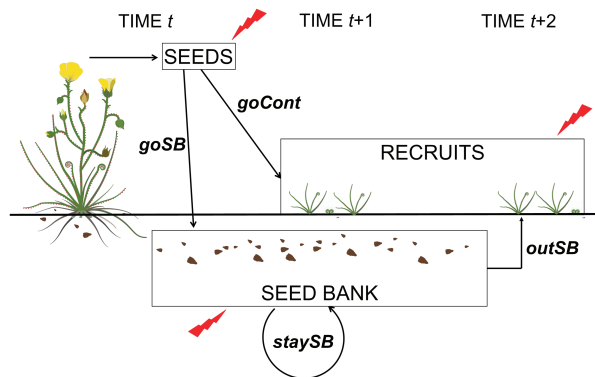


Figure 1. Possible fates of seeds after maturation at time t in the studied species *Drosophyllum lusitanicum*. Mature seeds either germinate and become established as recruits (*goCont*) the growing season following maturation in $t+1$ or enter the persistent seed bank (*goSB*). Once in the seed bank, seeds may either survive another year without germinating (*staySB*) or germinate (*outSB*) at $t+2$, or in later years. Mortality of seeds or seedlings before establishment is indicated by red lightning bolts and was only estimated from data for seeds before they reach soil.

Demographic data

We parameterized integral projection models (IPMs) with census and experimental field and laboratory data. We estimated vital rates of individuals with above-ground biomass from five annual censuses (2011–2015) comprising a total of 1371 individuals from five populations spanning the distribution range of *Drosophyllum* in southwestern Spain. The populations differed with respect to the time since last fire of the habitat (TSF, hereafter), being two, four, six, 10 and 29 years in 2015 (see Table A2.1 in Supplementary material Appendix 2 for details on TSF for all site–year combinations). Vital rates included survival (σ), growth (γ), probability of flowering (ϕ_0), number of flowering stalks (ϕ_1), number of flowers per stalk (ϕ_2), number of seeds per flower (ϕ_3), and seedling size distribution the next year (ϕ_4) (Supplementary material Appendix 2). The IPM's state variable for its continuous component was $size = \log(\text{no. of leaves} \times \text{length of longest leaf (cm)})$, after model selection for σ , γ , ϕ_0 and ϕ_1 . We also quantified above-ground seed survival from the demographic census data in each population and year as $\sigma_s = 1 - \text{flower damage}$ (Supplementary material Appendix 2). We then used this parameter to modify vital rates describing seed production (ϕ_0 , ϕ_1 , ϕ_2 , ϕ_3 and ϕ_4).

We performed two three-year field seed burial experiments and a greenhouse germination trial, overall using > 5100 seeds, to quantify the possible fates of seeds – including seeds in the seed bank, the discrete component in the IPM (Fig. 1). Details on all experiments can be found in Supplementary material Appendix 2. Both field experiments were initiated in September 2012 and 2013, when reproductive *Drosophyllum* individuals release seeds. In one experiment, we randomly collected seeds from five populations and buried mesh bags containing 20 seeds each in recently burned and adjacent unburned heathland patches. We then dug out mesh bags 18 months after burial to estimate seed seed-bank stasis (*staySB*), which consisted of two probabilities: surviving and not germinating from the seed bank (Fig. 1). We assumed that the proportion of viable seeds encountered after 18 months corresponded to stasis within one time interval in the IPMs (one year), ensuring that seed-bank dynamics were at the same time scale as the rest of the species' life cycle modeled (Supplementary material Appendix 2). In a separate experiment, using the same design as in the mesh-bag burial experiment, we sowed 50 seeds < 1 cm below the soil surface. We recorded germination 6 and 18 months after sowing to estimate, respectively, immediate seedling establishment, i.e. the probability of establishment in the spring following seed dispersal (*goCont*), and the probability of establishment, or egression, from the seed bank at least two springs after dispersal (*outSB*; Fig. 1). The vital rate *outSB* consisted of two probabilities that we could not separate: seedling emergence and survival to establishment (Fig. 1). We defined the proportion of seeds entering the seed bank (*goSB*) as $1 - goCont - \omega_s$, where ω_s = seedling mortality prior to the census, i.e. seedlings that emerged four months after sowing but failed to establish (Supplementary material Appendix 2). Lastly, in greenhouse trials, we exposed seeds to heat and smoke treatments and quantified germination, which we used as a proxy for seed-bank egression after fires (*outSB* in TSF₀). Similarly, seed-bank stasis after fire was estimated from an examination

of *Drosophyllum* seeds in soil samples from recently burned patches (Supplementary material Appendix 2).

Model parameterization

We used a Bayesian framework to fit all vital-rate models because of its advantages over frequentist approaches, including straightforward inclusion of spatial and temporal variation and ease of uncertainty simulation (Evans et al. 2010, Elderd and Miller 2016).

We modeled the above-ground vital rates as functions of size using generalized linear mixed models (GLMMs). To account for environmental variability in vital rates, we included TSF as a covariate in all vital-rate models. As heathland habitats > 3 years after fire do not change significantly in species composition and structure, we organized TSF into a categorical variable consisting of 1, 2, 3 or > 3 years since fire. IPMs for TSF₀ (burning) consisted of stasis in and germination from the seed bank, with 0 transition probabilities elsewhere, reflecting the death of above-ground individuals by fire. Using the deviance information criterion (DIC), we chose the most plausible model for each vital rate (Table 1; see Supplementary material Appendix 3 for all candidate models). The best-fit models describing growth (γ) and probability of flowering (ϕ_0) were defined as

$$g(\mu_{(i)}) = \alpha_0 + \alpha_{j(i)} + \beta_c \times size_{(i)} + \beta_{jc} \times size_{(i)} + \alpha_{s(i)} \quad (1)$$

where $g()$ is the link function applied to the likelihood distribution of the response μ for each individual i ; α_0 is the model intercept; α_j is the mean response at each TSF level j , compared with the model intercept; β_c is the overall slope for $size$; β_{jc} is the change of the $size$ slope at each TSF level j ; and α_s is the random effect on the model intercept for each site s (Table 1). Ideally, both random temporal and spatial variation should have been included, but our data did not offer enough degrees of freedom, as year \times site interactions are confounded with TSF effects. In our models we used only spatial variation. Sites were chosen to span the topographic gradient for our species (Supplementary material Appendix 2). $Size \times TSF$ interactions (β_{jc}) were not significant for survival (σ), the number of stalks (ϕ_1), and number of flowers per stalk (ϕ_2), so these models contain only additive effects (Table 1). No data were available to link seedling size in time $t + 1$ to parent size in t , and we therefore excluded the β parameters, keeping all other aspects of the general model design (Eq. 1, Table 1). Number of seeds per flower (ϕ_3) was treated as a constant in all models as it did not depend on size or TSF (likelihood ratio test, $D = 1.4$, $DF = 1$).

Vital rates related to seed-bank transitions (*goSB*, *staySB* and *outSB*, Table 1) were defined as binomial functions of the post-fire status of experimental patches (arranged as blocks), $\alpha_{p(r)}$, for each replicate r , where p could be either burned or unburned, and a random block effect, α_b :

$$g(\mu_{(r)}) = \alpha_0 + \alpha_{p(r)} + \alpha_{b(r)} \quad (2)$$

The predictions obtained from Eq. 2 were then associated with different TSF categories, assuming that the fixed effects of models for the three seed-bank vital rates in burned and unburned patches represented dynamics in TSF_{1,2} and TSF_{3,>3}, respectively (Table 2).

Table 1. Parameterization of the models used to describe vital rates of *Drosophyllum lusitanicum*. The models shown described the data best among several candidate models. Superscripts indicate the names of parameters in the R scripts (Supplementary material Appendix 1). The distributions B, \mathcal{N} , and NB correspond to the Bernoulli, normal, and negative binomial distribution, respectively. TSF – time since last fire. PFS – post-fire habitat status. Δ DIC indicate the difference in values between the chosen model and the second-best model with fewer parameters, which could be a – intercept-only; b – size only; c – size + TSF. See main text and Supplementary material Appendix 3 for detail.

Vital-rate model	Parameters	Link function	Likelihood distribution	Δ DIC
Survival (σ)	$\mu^{\text{surv}} = \alpha_0^{\text{surv}} + \alpha_j^{\text{surv}}[\text{TSF}] + \beta_c^{\text{surv}} \times \text{size} + \alpha_s^{\text{surv}}[\text{site}]$	logit(σ)	$\sigma \sim B(\mu^{\text{surv}})$	-432.0 ^b
Growth (γ)	$\mu^{\text{gr}} = \alpha_0^{\text{gr}} + \alpha_j^{\text{gr}}[\text{TSF}] + (\beta_c^{\text{gr}} + \beta_{jc}^{\text{gr}}) \times \text{size} + \alpha_s^{\text{gr}}[\text{site}]$	none	$\gamma \sim \mathcal{N}(\mu^{\text{gr}}, \tau^{\text{gr}})$	-5.0 ^c
Probability of flowering (ϕ_0)	$\mu^{\text{fl}} = \alpha_0^{\text{fl}} + \alpha_j^{\text{fl}}[\text{TSF}] + (\beta_c^{\text{fl}} + \beta_{jc}^{\text{fl}}) \times \text{size} + \alpha_s^{\text{fl}}[\text{site}]$	logit(ϕ_0)	$\phi_0 \sim B(\mu^{\text{fl}})$	-9.0 ^c
Number of flowering stalks (ϕ_1)	$\mu^{\text{fs}} = \alpha_0^{\text{fs}} + \alpha_j^{\text{fs}}[\text{TSF}] + \beta_c^{\text{fs}} \times \text{size} + \alpha_s^{\text{fs}}[\text{site}]$	log(ϕ_1)	$\phi_1 \sim \text{NB}(\rho^{\text{fs}}, \mu^{\text{fs}})$	-7.0 ^b
Number of flowers per stalk (ϕ_2)	$\mu^{\text{fps}} = \alpha_0^{\text{fps}} + \alpha_j^{\text{fps}}[\text{TSF}] + \beta_c^{\text{fps}} \times \text{size} + \alpha_s^{\text{fps}}[\text{site}]$	log(ϕ_2)	$\phi_2 \sim \text{NB}(\rho^{\text{fps}}, \mu^{\text{fps}})$	-5.0 ^b
Seedling size (ϕ_4)	$\mu^{\text{sds}} = \alpha_0^{\text{sds}} + \alpha_j^{\text{sds}}[\text{TSF}] + \alpha_s^{\text{sds}}[\text{site}]$	none	$\phi_3 \sim \mathcal{N}(\mu^{\text{sds}}, \tau^{\text{sds}})$	-20.0 ^a
Immediate germination (<i>goCont</i>)	$\mu^{\text{goCont}} = \alpha_0^{\text{goCont}} + \alpha_p^{\text{goCont}}[\text{PFS}] + \alpha_b^{\text{goCont}}[\text{block}]$	logit(<i>goCont</i>)	<i>goCont</i> $\sim B(\mu^{\text{goCont}})$	-38.2 ^a
Stasis is seed bank (<i>staySB</i>)	$\mu^{\text{staySB}} = \alpha_0^{\text{staySB}} + \alpha_p^{\text{staySB}}[\text{PFS}] + \alpha_b^{\text{staySB}}[\text{block}]$	logit(<i>staySB</i>)	<i>staySB</i> $\sim B(\mu^{\text{staySB}})$	-6.8 ^a
Egression from seed bank (<i>outSB</i>)	$\mu^{\text{outSB}} = \alpha_0^{\text{outSB}} + \alpha_p^{\text{outSB}}[\text{PFS}] + \alpha_b^{\text{outSB}}[\text{block}]$	logit(<i>outSB</i>)	<i>outSB</i> $\sim B(\mu^{\text{outSB}})$	-206.0 ^a

IPM construction

In order to associate environmental (post-fire) states with vital rates in stochastic simulations, we built IPMs for each combination of TSF and site-effect estimates. The IPMs consisted of two coupled equations integrated over $L = 0$ and $U = 9.6$ sizes x at t to give a vector of sizes y at $t + 1$. The lower and upper integration limits corresponded to the minimum observed size (individual with one, 1-cm long leaf) and $1.1 \times$ maximum observed size, respectively. The first of the two equations describes the composition of the seed bank (S) at $t + 1$ through the contribution of seeds produced by above-ground individuals (*goSB*) and dormant seeds remaining in the seed bank (*staySB*) at t :

$$S(t+1) = S(t)\text{staySB} + \int_L^U \varphi_0(x)\varphi_1(x)\varphi_2(x)\varphi_3\sigma_5\text{goSBn}(x,t)dx \quad (3)$$

The second equation describes the dynamics of above-ground individuals through emergence and establishment of seedlings from the seedbank, survival of established individuals, and contributions of seedlings by reproductive individuals the previous year:

$$n(y,t+1) = S(t)\text{outSB}\varphi_3(y) + \int_L^U [\sigma(x)\gamma(y,x) + \varphi_0^-(x)\varphi_1(x)\varphi_2(x)\varphi_3\sigma_5\text{goCont}\varphi_4(y)n(x,t)dx \quad (4)$$

Table 2. Extrapolation of seed-related vital rates calculated from field experiments to time since fire (TSF) categories used to build integral projection models (IPMs) for *Drosophyllum lusitanicum*. The four vital rates estimated in *burned* (B) and *unburned* (U) heathland patches (see methods) were modeled as binomial functions (Table 1); Constant values (\dagger) of vital rates in some TSF categories were obtained from soil seed bank censuses (*staySB* in $\text{TSF}_{0,1}$), a greenhouse germination trial (*outSB* in TSF_0), measurements of seedling mortality (*goSB* in $\text{TSF}_{2,3,>3}$), or censuses of actual field germination (c; Supplementary material Appendix 2 for details); σ_5 is seed survival in $\text{TSF}_{2,3,>3}$.

	TSF_0	TSF_1	TSF_2	TSF_3	$\text{TSF}_{>3}$
Immediate germination (<i>goCont</i>)	0	0	$\sigma_{S2} \times \text{goCont_U} \times c^\dagger$	$\sigma_{S3} \times \text{goCont_U} \times c^\dagger$	$\sigma_{S>3} \times \text{goCont_U} \times c^\dagger$
Ingression into seed bank (<i>goSB</i>)	0	0	$\sigma_{S2} \times (1 - \text{goCont_U} - 0.03^\dagger)$	$\sigma_{S3} \times (1 - \text{goCont_U} - 0.03^\dagger)$	$\sigma_{S>3} \times (1 - \text{goCont_U} - 0.03^\dagger)$
Stasis in seed bank (<i>staySB</i>)	0.1 [†]	0.05 [†]	<i>staySB</i> _B	<i>staySB</i> _U	<i>staySB</i> _U
Egression from seed bank (<i>outSB</i>)	0.81 [†]	<i>outSB</i> _B	<i>outSB</i> _B $\times c^\dagger$	<i>outSB</i> _U $\times c^\dagger$	<i>outSB</i> _U $\times c^\dagger$

Parameter uncertainty

We used MCMC sampling to estimate the distributions of all 99 model parameters quantifying vital rates. In all models, we used normal ($\mu = 0$; $1/\theta^2 = 1 \times 10^{-06}$) or uniform uninformative priors for most fixed factors. The posterior sampling was based on 100 000 iterations, after a burn-in of 100 000 steps, using four chains and subsampling every 400th simulated value (see Supplementary material Appendix 3 for details on all priors and MCMC sampling procedures). We therefore obtained the parameter distributions for *goSB*, *staySB* and *outSB* from 1000 samples of the joint posterior distribution of the parameters α_0 and $\alpha_{p(t)}$ (Eq. 2). The full Bayesian models and application of MCMC convergence diagnostics can be found in the R script `BayModel.R` in the Supplementary material Appendix 1. We ran all MCMC simulations in OpenBUGS ver. 3.2.3 using the R package BRugs to create an R interface to OpenBUGS (Thomas et al. 2006).

Stochastic simulations of population dynamics

We built the TSF-site specific IPMs for each posterior parameter sample ($n = 1000$) associated with the vital rates describing seed-bank transitions: ingression into (*goSB*), stasis (*staySB*), egression from the seed bank (*outSB*), and both *staySB* and *outSB*. We sampled parameters for seed-bank stasis and egression independently because seeds that

do not stay in the seed bank may die before successful establishment, i.e. $outSB \neq 1 - staySB$ (Fig. 1). We kept the remaining vital rate parameters at their average posterior values to assess effects of parameter uncertainty on estimates of population viability of seed-bank related vital rates only (see `makeIPM.R` in Supplementary material Appendix 1).

For each parameter sample, we ran 100 simulations of stochastic population projections to assess population viability under a naturally occurring range of fire return intervals for the study region (Ojeda 2009): 10 to 100 years at 10-year increments (Fig. 2). At each fire return interval, we defined TSF transitions as a Markov-chain process with states corresponding to the five TSF categories: 0, 1, 2, 3 and >3 years after fire and transitions between states corresponding to fire probability = $1/\text{fire return interval}$ (Fig. 2). Each of 100 simulations for a given fire return interval initiated with an IPM depicting TSF_0 , and population dynamics were projected for $t = 4000$ years after discarding the initial 500 iterations (Fig. 2). At each iteration, one of five

site IPMs at a given TSF state was randomly chosen, while the sequence of TSF states during the iterations was determined by the Markov-chain process (Fig. 2). For each simulation, we calculated the stochastic population growth rate, $\log \lambda_s$ (Caswell 2001, Eq. 14.61). Scripts for the simulations of population viability are available in `sLambdaSimul.R` and `sLambdaRmpi.R` for implementation using parallel processing.

Our simulations therefore produced two nested levels of $\log \lambda_s$ estimates obtained from 1) 1000 samples of parameters, and 2) 100 simulations of population projections within each parameter sample (Fig. 2). Differences in $\log \lambda_s$ among parameters represented parameter uncertainty while differences among the 100 simulations represented environmental variability. The latter variability consisted of both between-state (picking IPMs corresponding to different TSF categories at each iteration) and within-state (picking a site from the random effect estimates at each iteration) variability. We quantified the contribution of parameter uncertainty

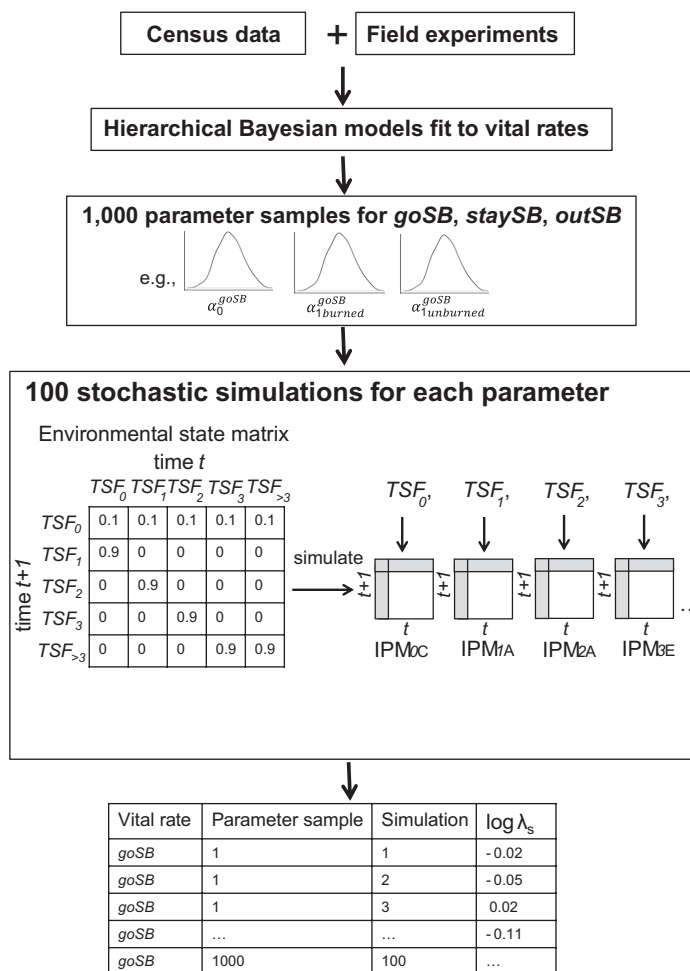


Figure 2. Hierarchical structure of simulations of the stochastic population growth rate, $\log \lambda_s$, incorporating parameter uncertainty of three vital rates: seed-bank ingress (*goSB*), stasis (*staySB*), and egression (*outSB*; Fig. 1). Bayesian posterior distributions were sampled to obtain 1000 parameters for each vital rate. For each parameter, $\log \lambda_s$ were simulated from 100 stochastic projections, each run over 4000 discrete time steps t using Markov chain transitions between five time-since-fire (TSF) environments (0, 1, 2, 3, >3). The transitions depended on 10 fire return intervals (here 0.1 probability of burning corresponds to 1 fire in 10 years). Each environmental TSF state was associated with five IPMs, one for each site (A–E) modeled in the study. The first row and column of IPMs (grey) depict seed-bank transitions. Differences in $\log \lambda_s$ estimates among the 1000 parameter samples and 100 stochastic projections depicted parameter uncertainty and environmental variability, respectively.

to variation in $\log \lambda_s$, by fitting a GLMM to the estimates of $\log \lambda_s$ at each fire return interval treating the posterior parameters as a random effect (Evans et al. 2010). Lastly, we compared the distribution of $\log \lambda_s$ estimates when incorporating parameter uncertainty to estimates based on environmental variability only. We obtained the latter by calculating $\log \lambda_s$ for 100 simulations using IPMs built from average parameter samples for each TSF category (`makeIPM.R` in Supplementary material Appendix 1).

From the mean and variance of the 100 $\log \lambda_s$ estimates at each posterior parameter sample and fire return interval, we analytically obtained the probability of quasi-extinction $P_q(t)$ at $t = 50$ and 100 years as described in Trotter et al. (2013). We chose the extinction threshold to be 0.01, i.e. populations were considered extinct when population sizes (including seeds in the seed bank) fell to 1% of current population sizes (Quintana-Ascencio et al. 2003).

In order to compare the effects of changes in *goSB*, *staySB* and *outSB* on $\log \lambda_s$, relative to other vital rates, at different fire-return intervals, we perturbed each vital rate used to compose the IPMs by its mean, μ , and standard deviation, σ , across all environmental states (see `perturbVR.R` in Supplementary material Appendix 1). We then used the chain rule to calculate 1) how these perturbations affected the IPM kernels, and 2) how the latter in turn affected $\log \lambda_s$. These calculations provided us with elasticities, E^μ and E^σ of $\log \lambda_s$ to changes in the mean and variance of vital rates, respectively (Tuljapurkar et al. 2003, Haridas and Tuljapurkar 2005, Supplementary material Appendix 4). Unlike deterministic elasticities however, E^μ and E^σ do not sum to one and thus do not provide a measure of relative contribution (Haridas and Tuljapurkar 2005). To calculate the relative elasticities focusing on changes in the mean of each vital rate, we therefore divided the E^μ for each vital rate, for example *staySB*, summed over all affected IPM kernel entries, j , by the total E , summed over E^μ and E^σ for all vital rates, vr , (Morris et al. 2008):

$$\frac{\sum_j E_{staySBj}^\mu}{\sum_i (E_{vri}^\mu + E_{vri}^\sigma)} \quad (5)$$

We used mean parameter values and a subset of five fire return intervals, 10, 30, 50, 80 and 100 years, to calculate the elasticities. As *Drosophyllum* is a post-fire dwelling, short-lived species with vital-rate variation governed by post-fire habitat succession, we did not consider intrinsic demographic tradeoffs, for example between reproduction and growth (Miller et al. 2012), in the elasticity calculations.

Data deposition

Data available from the Dryad Digital Repository: <<http://dx.doi.org/10.5061/dryad.rq7t3>> (Paniw et al. 2016).

Results

Importance of seed-bank vital rates for stochastic population dynamics

Seed-bank stasis (*staySB*) and egression (*outSB*; Fig. 1) had the largest relative effects on the stochastic growth rate, \log

λ_s , of *Drosophyllum* populations across fire return intervals (Fig. 3). In particular, changing the average of *staySB* produced the highest relative elasticities, E^μ , among all vital rates (0.5 at fire return interval of 100 years), followed by *outSB*. For both vital rates, relative E^μ increased with fire return interval (Fig. 3). Ingression into the seed-bank, *goSB*, had relatively low E^μ , remaining approx. 0.05 across the five fire return intervals simulated.

Influence of parameter uncertainty on estimation of population growth and extinction

In all simulations, average $\log \lambda_s$ decreased monotonically with increasing fire return interval (Spearman's $\rho = -1$), while $P_q(t)$ increased with increasing fire return interval (Fig. 4, 5). In simulations using mean parameter values, $\log \lambda_s$ variance decreased with increasing fire return interval because fewer TSF states (largely $TSF < 3$) were sampled at each iteration with burning becoming less likely (Fig. 4). However, when uncertainties in *staySB*, *outSB*, or both were incorporated into simulations, estimates of $\log \lambda_s$ were more variable compared to simulations based on mean parameters, and their variation increased with increasing fire return (Fig. 4). Accordingly, the proportion of variation among the 100 000 $\log \lambda_s$ estimates attributed to parameter uncertainty varied across fire return intervals and vital rates sampled, being < 0.01 for *goSB* and increasing from > 0.1 at 10 years to > 0.7 at 100 years return interval for *staySB* and *outSB* (Fig. 4, Supplementary material Appendix 4 Table A4.2). The largest contribution of parameter uncertainty was obtained when including samples of both *staySB* and *outSB* into simulations (Supplementary material Appendix 4 Table A4.2).

The high uncertainty in the estimates of $\log \lambda_s$ at increasing fire return intervals influenced potential inferences about population viability. Whereas the 100 projections of $\log \lambda_s$, based on environmental variability alone (grey boxplots in

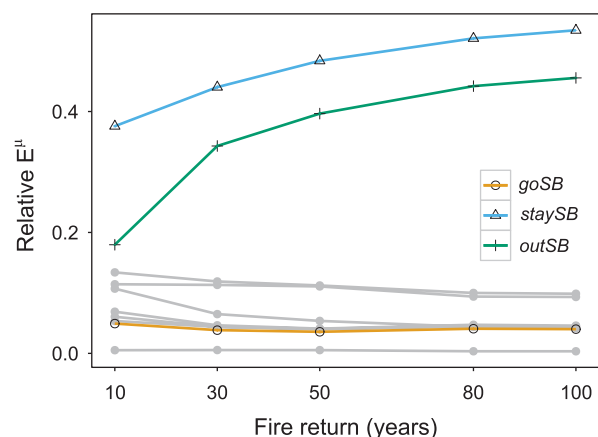


Figure 3. Seed-bank vital rates govern the population dynamics of *Drosophyllum*, regardless of fire return interval. Elasticities of the stochastic population growth rate, $\log \lambda_s$, to changes in the mean, E^μ , of seed-bank stasis (*staySB*) and egression (*outSB*) are higher compared with other vital rates (filled grey points and lines) at five simulated fire return intervals: 10, 30, 50, 80 and 100 years. SE around the relative E^μ obtained from 100 simulations were $< 1 \times 10^{-03}$.

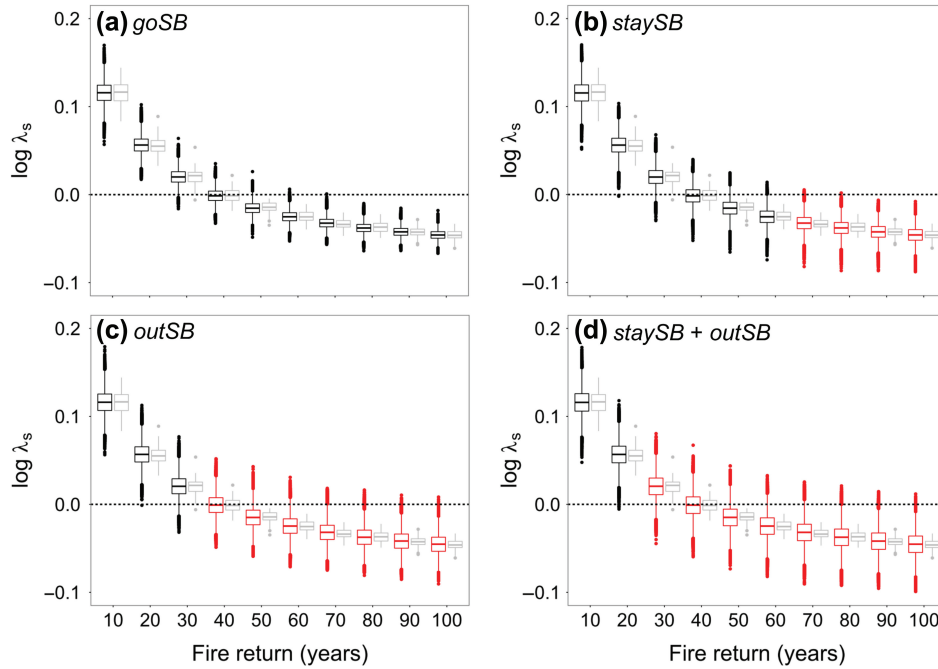


Figure 4. Parameter uncertainty contributes significantly to variation of simulated stochastic population growth rate estimates ($\log \lambda_s$). Box-and-whisker plots display $\log \lambda_s$ as function of fire return interval (x-axis). At each fire return interval, the black and red box plots summarize the variation among 100 000 $\log \lambda_s$ obtained from 100 stochastic projections of $\log \lambda_s$ for each of 1000 posterior parameter samples describing (a) seed-bank ingress (*goSB*), (b) stasis (*staySB*), (c) egression (*outSB*), and (d) both *staySB* and *outSB*. Red box plots indicate a proportional contribution of parameter uncertainty to the variation in $\log \lambda_s > 50\%$. Grey box plots in (a)–(d) summarize variation in $\log \lambda_s$ estimates from 100 stochastic simulations using mean parameter values for all vital rates. Black horizontal dashed lines indicate stable population sizes.

Fig. 4) showed a clear decline in viability at a fire return interval of ≥ 50 years, high uncertainty associated with these projections meant that the certainty in the threshold of 50 years (fire return interval) was relatively low (Fig. 4). In fact, uncertainty in $P_q(t)$ markedly increased when accounting for parameter uncertainty in *staySB* and *outSB*. Compared with estimates based on mean parameter values, $P_q(t)$ could be > 20 percentage points higher or lower under particular combinations of *staySB* and *outSB* (Fig. 5). The strongest effects of parameter uncertainty appeared at $t = 100$ years, where $P_q(t)$ as high as 0.77 cannot be ruled out at a fire return interval of 100 years (Fig. 5b).

Discussion

Dormant life stages such as larvae in diapause, some spores, or seeds in permanent seed banks are believed to play key roles in the adaption of species to environmental stochasticity (Benton and Grant 1996, Smallegange and Coulson 2013). Demographic information on these life stages, however, is often limited (Doak et al. 2002). When incorporating such data in population models, the parameter uncertainty in vital rates describing dormant life stages must be quantified in order to separate sources of variability for measures such as extinction or invasion risk or the stochastic population

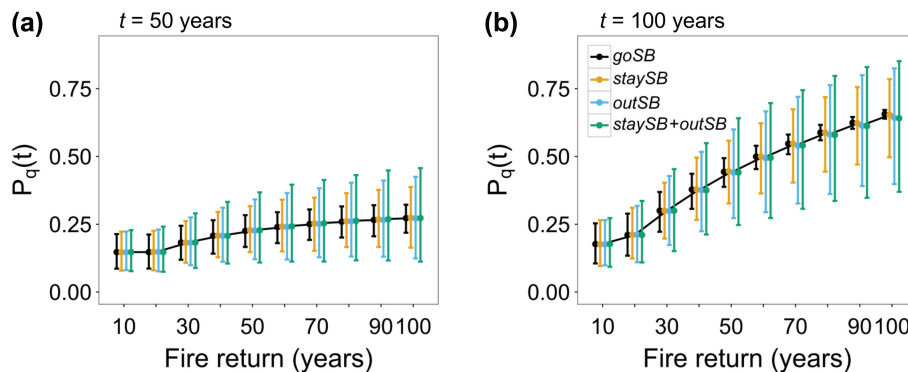


Figure 5. Increases in the probability of quasi-extinction, $P_q(t)$, at $t = 50$ or 100 years as function of fire return interval. The extinction threshold was assumed to be 0.01. At each fire return, $P_q(t)$ was calculated from the mean and variance of 100 stochastic growth rates obtained for each of 1000 posterior parameter samples describing seed-bank ingress (*goSB*), stasis (*staySB*), egression (*outSB*), and both *staySB* and *outSB* (different colors in plot). Points represent $P_q(t)$ averaged over the 1000 parameter samples. Error bars show $\pm 95\%$ non-parametric quantile CI (2.5 and 97.5 quantile) obtained from the $P_q(t)$ for each of the 1000 parameter samples.

growth rate, $\log \lambda_s$ (Ellner and Fieberg 2003, Evans et al. 2010, Lee et al. 2015). Here we provide evidence that uncertainty around vital-rate parameters describing critical seed-bank transitions of a fire-adapted plant may translate into large uncertainty in the estimates of population-level parameters, and omitting it can seriously bias interpretation of population performance. The Bayesian framework we employed to quantify parameter uncertainty was developed by Evans et al. (2010) for matrix population models and recently extended to IPMs by Elder and Miller (2016). Our study provides an important extension to the work by Elder and Miller – the explicit consideration of discrete, dormant stages and categorical covariates (TSF) when constructing Bayesian IPMs, simulating stochastic environmental transitions, and quantifying contributions of parameter uncertainty to population dynamics.

The role of the seed bank for population dynamics

Our results showed that life-cycle transitions related to the seed bank (Fig. 1) strongly influence population dynamics of the fire-adapted *Drosophyllum lusitanicum*. Seed-bank stasis can ensure population persistence when above-ground individuals cannot survive in long-unburned habitats (Menges and Quintana-Ascencio 2004, Adams et al. 2005); while large egression events after fires and periodic egression into favorable microhabitats in unburned stands result in growth of above-ground individuals, which replenish the seed bank (Quintana-Ascencio et al. 2003, Paniw et al. 2015). Our elasticity analyses suggested that increases in both seed-bank stasis and egression would strongly, positively affect the stochastic population growth rate (Fig. 3). However, these two vital rates are negatively correlated, implying that seed-bank stasis can only be optimized at the expense of egression and vice versa (Benton and Grant 1996). At long fire return intervals, an increase in the importance of seed-bank stasis has been shown in other studies (Quintana-Ascencio et al. 2003, Menges and Quintana-Ascencio 2004) and would likely be more critical for *Drosophyllum* populations than egression. This is because egression is highly dependent on open microhabitats being created in unburned habitats, which occurs irregularly and on a small scale in natural heathlands (Paniw unpubl.). On the other hand, changes in seed-bank ingression affected population growth far less than either seed-bank stasis or egression. This vital rate varied little across time-since-fire habitats (Supplementary material Appendix 2), and vital rates related to above-ground fecundity have a stronger effect on population dynamics, which has been demonstrated for a number of disturbance-adapted, early colonizing species (Silvertown et al. 1996, Smith et al. 2005).

Parameter uncertainty in dormant life stages and inference about population dynamics

Quantifying parameter uncertainty of vital rates with strong effects on population growth can help researchers to account for the uncertainty in the effect of environmental processes on stochastic population dynamics (Evans et al. 2010). For *Drosophyllum*, parameter uncertainty related to seed-bank stasis and egression explained up to 79% of $\log \lambda_s$ variation among our 100 000 simulations. Overall, the uncertainty

around estimates of both $\log \lambda_s$ and $P_q(t)$ increased with fire-return interval modeled. This occurred mainly because seed-bank dynamics become more important for persistence of a fire-adapted species in the absence of fires (Quintana-Ascencio et al. 2003), with uncertainty in their estimates increasingly affecting the accuracy with which population dynamics can be assessed. Therefore, with limited data on seed-bank dynamics in the case of *Drosophyllum* and many other species (Baskin and Baskin 1998), a robust interpretation of viability analyses in long unburned populations relies primarily on the incorporation of parameter uncertainty into population analyses. Meanwhile, interpretations about the role of environmental processes themselves (e.g. fire regimes) become increasingly uncertain when projecting data-limited population dynamics into the future (Boyce et al. 2006).

With high potential for errors in the estimates of population dynamics for species with limited demographic data, uncertainty analyses can become critical when defining management strategies (Hunter et al. 2010). Fire is of vital importance for *Drosophyllum*, a species that reaches full reproductive potential within the first 2–4 post-fire years in natural Mediterranean heathlands (Correia and Freitas 2002) and then mostly persists in the seed bank until the next fire or disturbance occurs (Paniw et al. 2015). However, current fire return intervals in the Mediterranean have increased due to fire suppression (Ojeda 2009, Turco et al. 2016), threatening population viability (Paniw et al. 2015). At fire return intervals of ≥ 50 years, which is still within the upper range of natural fire regimes across Mediterranean heathlands (Ojeda 2009, Plan INFOCA 2012), the mean estimates of $\log \lambda_s < 0$, implying population decline. However, the variation around this mean attributed to parameter uncertainty in *staySB* and *outSB* indicates that *Drosophyllum* populations may be able to persist with a fire return interval of about 60 years, and some even with a fire return interval of up to 70 years. For conservation management of this species, which may include prescribed burning or controlling for factors that may jeopardize survival of dormant seeds in the seed bank (Paniw et al. 2015), the accurate estimation of parameter uncertainty may directly define the heathlands considered for management depending on time since last fire. As population growth of *Drosophyllum* showed non-zero elasticities to changes in the remaining vital rates (Fig. 4) and given the large number of parameters estimated in our models, including samples of all parameters into the simulations would further increase the uncertainty of $\log \lambda_s$ and $P_q(t)$ estimates (Evans et al. 2010, Supplementary material Appendix 4). However, our aim here was to emphasize that interpretations of long-term stochastic population dynamics may strongly depend on quantification of a few critical vital rates and their uncertainties.

Implications of uncertainty for other life histories

Studies of other species with adaptations to buffer environmental stochasticity may also benefit from a better understanding of different sources of uncertainty, particularly under the emerging threats of climate change. In plants, vegetative dormancy may be as difficult to estimate as seed dormancy (Lesica and Crone 2007) but can play a critical role in buffering populations from stress, either physical

(Shefferson et al. 2005) or climatic (Salguero-Gómez et al. 2012). Likewise, in many insects, prolonged diapause can spread adult survival over several years but may be difficult to estimate (Solbreck and Widenfalk 2012). Whether and how such strategies may continue to buffer populations under human-induced disturbance and climatic changes is an emerging question (Boyce et al. 2006, Radchuk et al. 2013). An equally important question may be how to account for the inherent uncertainty due data-limited vital rates when assessing the significance of climatic variables on changes in population dynamics (Elder and Miller 2016).

Within a given life cycle, the quantification of parameter uncertainty may also be important for the estimates of correlated vital rates. Uncertainties in egression of seeds from the seed bank may for example influence estimates of recruitment (Eager et al. 2014). In *Drosophyllum*, recruitment is dependent on the environment and not so much on plant density. However, many species with persistent seed banks may exhibit a negative density dependence of seedling establishment (Eager et al. 2014). Here, uncertainty in the number of recruits from the seed bank may propagate to uncertainties in above-ground vital rates. In other organisms, responses to stress such as vegetative dormancy may have future consequences on fitness, e.g. lower growth as above-ground individual (Gremer et al. 2012). As such, large variation in the estimates of dormancy may directly influence the estimates of several other vital rates once individuals emerge above-ground. Studies of population dynamics encounter many types of covariation in vital rates (Tuljapurkar 1990, Morris et al. 2008), and the potential propagation of uncertainty throughout different vital rates has received little attention in plant demography as opposed to animal demography (Hunter et al. 2010, Lee et al. 2015).

Conclusions

Increasingly sophisticated methods are being used to address ecological and evolutionary questions regarding environmental stochasticity (Salguero-Gómez and de Kroon 2010, Low-Décarie et al. 2014). Population models have also gained complexity and realism in the last decades, allowing for more reliable analysis of population dynamics by accounting for different sources of variation in underlying vital-rate regressions (Evans et al. 2010, Merow et al. 2014, Tye et al. 2016). Here, we have contributed to this important body of literature by showing that, when dealing with dormant life-cycle stages with limited field data, stochastic models may gain robustness in the interpretation of projected population dynamics by including parameter uncertainty around vital rate means. An exhaustive sensitivity analysis to parameter uncertainty may strongly influence conservation management decisions, and we encourage population ecologists to explicitly address such uncertainties in their modeling approaches.

Acknowledgements – We are grateful to M. Gil-López, M. Scott, and M. Collado-Aliaño for logistical support during the data collection, to V. González-Ortiz *Drosophyllum* illustrations, and A. Jiménez's CITI team (UCA) for access to parallel processing.

Funding – This study has been financed by project BREATHAL (CGL2011-28759/BOS; Spanish *Ministerio de Economía y Competitividad*) to FO and RSG. MP was supported by a FPI

scholarship granted by the Spanish *Ministerio de Economía y Competitividad*, RSG by the Australian Research Council (DE140100505), the Max Planck Institute for Demographic Research and a NERC IRF NE/M018458/1, and PFQA by NSF-DEB 1347247 and NSF-DEB 0812753.

References

- Adams, V. M. et al. 2005. Importance of the seed bank for population viability and population monitoring in a threatened wetland herb. – *Biol. Conserv.* 124: 425–436.
- Baskin, C. C. and Baskin, J. M. 1998. Seeds: ecology, biogeography and evolution of dormancy and germination. – Academic Press.
- Benton, T. G. and Grant, A. 1996. How to keep fit in the real world: elasticity analyses and selection pressures on life histories in a variable environment. – *Am. Nat.* 147: 115–139.
- Boyce, M. S. et al. 2006. Demography in an increasingly variable world. – *Trends Ecol. Evol.* 21: 141–148.
- Calvo, L. et al. 2002. The dynamics of Mediterranean shrubs species over 12 years following perturbations. – *Plant Ecol.* 160: 25–42.
- Caswell, H. 2001. Matrix population models: construction, analysis and interpretation. – Sinauer.
- Cohen, D. 1966. Optimizing reproduction in a randomly varying environment. – *J. Theor. Biol.* 12: 119–129.
- Correia, E. and Freitas, H. 2002. *Drosophyllum lusitanicum*, an endangered west Mediterranean endemic carnivorous plant: threats and its ability to control available resources. – *Bot. J. Linn. Soc.* 140: 383–390.
- Doak, D. F. et al. 2002. Population viability analysis for plants: understanding the demographic consequences of seed banks for population health. – In: Beissinger, S. R. and McCullough, D. R. (eds), *Population viability analysis*. Univ. Chicago Press, pp. 312–337.
- Eager, E. A. et al. 2014. Modeling and analysis of a density-dependent stochastic integral projection model for a disturbance specialist plant and its seed bank. – *Bull. Math. Biol.* 76: 1809–1834.
- Easterling, M. R. et al. 2000. Size-specific sensitivity: applying a new structured population model. – *Ecology* 81: 694–708.
- Ehrlén, J. et al. 2016. Advancing environmentally explicit structured population models of plants. – *J. Ecol.* 104: 292–305.
- Elder, B. D. and Miller, T. E. 2016. Quantifying demographic uncertainty: Bayesian methods for integral projection models (IPMs). – *Ecol. Monogr.* 86: 125–144.
- Ellner, S. P. and Fieberg, J. 2003. Using PVA for management despite uncertainty: effects of habitat, hatcheries, and harvest on salmon. – *Ecology* 84: 1359–1369.
- Ellner, S. P. and Rees, M. 2006. Integral projection models for species with complex demography. – *Am. Nat.* 167: 410–428.
- Evans, M. E. et al. 2010. Fire, vital rates, and population viability: a hierarchical Bayesian analysis of the endangered Florida scrub mint. – *Ecol. Monogr.* 80: 627–649.
- Gioria, M. et al. 2012. Soil seed banks in plant invasions: promoting species invasiveness and long-term impact on plant community dynamics. – *Preslia* 84: 327–350.
- Gremer, J. R. and Venable, D. L. 2014. Bet hedging in desert winter annual plants: optimal germination strategies in a variable environment. – *Ecol. Lett.* 17: 380–387.
- Gremer, J. R. et al. 2012. Are dormant plants hedging their bets? Demographic consequences of prolonged dormancy in variable environments. – *Am. Nat.* 179: 315–327.
- Grime, J. P. 1977. Evidence for the existence of three primary strategies in plants and its relevance to ecological and evolutionary theory. – *Am. Nat.* 111: 1169–1194.

- Haridas, C.V. and Tuljapurkar, S. 2005. Elasticities in variable environments: properties and implications. – *Am. Nat.* 166: 481–495.
- Higgins, S. I. et al. 2000. Predicting extinction risks for plants: environmental stochasticity can save declining populations. – *Trends Ecol. Evol.* 15: 516–520.
- Honnay, O. et al. 2008. Can a seed bank maintain the genetic variation in the above ground plant population? – *Oikos* 117: 1–5.
- Hunter, C. M. et al. 2010. Climate change threatens polar bear populations: a stochastic demographic analysis. – *Ecology* 91: 2883–2897.
- Lee, A. M. et al. 2015. An integrated population model for a long-lived ungulate: more efficient data use with Bayesian methods. – *Oikos* 124: 806–816.
- Lesica, P. and Crone, E. E. 2007. Causes and consequences of prolonged dormancy for an iteroparous geophyte, *Silene spaldingii*. – *J. Ecol.* 95: 1360–1369.
- Low-Décarie, E. et al. 2014. Rising complexity and falling explanatory power in ecology. – *Front. Ecol. Environ.* 12: 412–418.
- Menges, E. S. 2000. Population viability analyses in plants: challenges and opportunities. – *Trends Ecol. Evol.* 15: 51–56.
- Menges, E. S. and Quintana-Ascencio, P. F. 2004. Population viability with fire in *Eryngium cuneifolium*: deciphering a decade of demographic data. – *Ecol. Monogr.* 74: 79–99.
- Merow, C. et al. 2014. Advancing population ecology with integral projection models: a practical guide. – *Meth. Ecol. Evol.* 5: 99–110.
- Miller, T. E. et al. 2012. Evolutionary demography of iteroparous plants: incorporating non-lethal costs of reproduction into integral projection models. – *Proc. R. Soc. B.* rspb20120326.
- Morris, W. F. et al. 2008. Longevity can buffer plant and animal populations against changing climatic variability. – *Ecology* 89: 19–25.
- Navarra, J. J. and Quintana-Ascencio, P. F. 2012. Spatial pattern and composition of the Florida scrub seed bank and vegetation along an anthropogenic disturbance gradient. – *Appl. Veg. Sci.* 15: 349–358.
- Ojeda, F. 2009. 4030 Brezales secos europeos. – In: Bases ecológicas preliminares para la conservación de los tipos de hábitat de interés comunitario en España. Ministerio de Medio Ambiente, y Medio Rural y Marino, pp. 1–66.
- Paniw, M. et al. 2015. Local-scale disturbances can benefit an endangered, fire-adapted plant species in Western Mediterranean heathlands in the absence of fire. – *Biol. Conserv.* 187: 74–81.
- Paniw, M. et al. 2016. Data from: Accounting for uncertainty in dormant life stages in stochastic demographic models. – Dryad Digital Repository, <<http://dx.doi.org/10.5061/dryad.rq7t3>>.
- Plan INFOCA 2012. Incendios forestales. – Junta de Andalucía: Consejería de Medioambiente y Ordenación del Territorio. <www.juntadeandalucia.es/medioambiente>
- Pozzi, A. C. et al. 2015. In-plant sporulation phenotype: a major life history trait to understand the evolution of *Alnus*-infective *Frankia* strains. – *Environ. Microbiol.* 17: 3125–3138.
- Quintana-Ascencio, P. F. et al. 2003. A fire-explicit population viability analysis of *Hypericum cumulicola* in Florida rosemary shrub. – *Conserv. Biol.* 17: 433–449.
- Radchuk, V. et al. 2013. Each life stage matters: the importance of assessing the response to climate change over the complete life cycle in butterflies. – *J. Anim. Ecol.* 82: 275–285.
- Rees, M. et al. 2006. Seed dormancy and delayed flowering in monocarpic plants: selective interactions in a stochastic environment. – *Am. Nat.* 168: E53–E71.
- Salces-Castellano, A. et al. 2016. Attract them anyway – benefits of large, showy flowers in a highly autogamous, carnivorous plant species. – *AoB Plants*, plw 017.
- Salguero-Gómez, R. and de Kroon, H. 2010. Matrix projection models meet variation in the real world. – *J. Ecol.* 98: 250–254.
- Salguero-Gómez, R. et al. 2012. A demographic approach to study effects of climate change in desert plants. – *Proc. R. Soc. B* 367: 3100–3114.
- Schiesari, L. and O'Connor, M. B. 2013. Diapause: delaying the developmental clock in response to a changing environment. – *Curr. Topics Dev. Biol.* 105: 213–246.
- Shefferson, R. P. et al. 2005. Adult whole-plant dormancy induced by stress in long-lived orchids. – *Ecology* 86: 3099–3104.
- Shen-Miller, J. et al. 1995. Exceptional seed longevity and robust growth: ancient sacred lotus from China. – *Am. J. Bot.* 82: 1367–1380.
- Silvertown, J. et al. 1996. Interpretation of elasticity matrices as an aid to the management of plant populations for conservation. – *Conserv. Biol.* 10: 591–597.
- Smallegange, I. M. and Coulson, T. 2013. Towards a general, population-level understanding of eco-evolutionary change. – *Trends Ecol. Evol.* 28: 143–148.
- Smith, M. et al. 2005. Stochastic flood and precipitation regimes and the population dynamics of a threatened floodplain plant. – *Ecol. Appl.* 15: 1036–1052.
- Solbreck, C. and Widenfalk, O. 2012. Very long diapause and extreme resistance to population disturbance in a galling insect. – *Ecol. Entomol.* 37: 51–55.
- Thomas, A. et al. 2006. Making BUGS Open. – *R News* 6: 12–17.
- Tielbörger, K. et al. 2012. Bet-hedging germination in annual plants: a sound empirical test of the theoretical foundations. – *Oikos* 121: 1860–1868.
- Trotter, M. V. et al. 2013. Beyond the mean: sensitivities of the variance of population growth. – *Meth. Ecol. Evol.* 4: 290–298.
- Tuljapurkar, S. 1990. Population dynamics in variable environments. – Springer.
- Tuljapurkar, S. et al. 2003. The many growth rates and elasticities of populations in random environments. – *Am. Nat.* 162: 489–502.
- Turco, M. et al. 2016. Decreasing fires in Mediterranean Europe. – *PLoS ONE* 11: e0150663.
- Tye, M. R. et al. 2016. A demographic ménage à trois: interactions between disturbances both amplify and dampen population dynamics of an endemic plant. – *J. Ecol.* 104: 1778–1788.
- Venable, D. L. 2007. Bet hedging in a guild of desert annuals. – *Ecology* 88: 1086–1090.

Supplementary material (available online as Appendix oik-03696 at <www.oikosjournal.org/appendix/oik-03696>). Appendix 1: overview of the R code provided in the manuscript. Appendix 2: details on demographic censuses and field experiments. Appendix 3: additional information on the modeling processes. Appendix 4: additional modeling results.